31st Annual International Conference of the IEEE EMBS
Minneapolis, Minnesota, USA, September 2-6, 2009

Magnetoencephalographic Imaging of Deep Corticostriatal Network Activity During a Rewards Paradigm

Eliezer Y. Kanal, Mingui Sun, Tolga E. Özkurt, Wenyan Jia, and Robert Sclabassi

Abstract— **The human rewards network is a complex system spanning both cortical and subcortical regions. While much is known about the functions of the various components of the network, research on the behavior of the network as a whole has been stymied due to an inability to detect signals at a high enough temporal resolution from both superficial and deep network components simultaneously. In this paper, we describe the application of magnetoencephalographic imaging (MEG) combined with advanced signal processing techniques to this problem. Using data collected while subjects performed a rewards-related gambling paradigm demonstrated to activate the rewards network, we were able to identify neural signals which correspond to deep network activity. We also show that this signal was not observable prior to filtration. These results suggest that MEG imaging may be a viable tool for the detection of deep neural activity.**

I. Introduction

The human reward processing system encompasses a number of neural regions, both deep and superficial. Among the regions involved are the striatum, the anterior cingulate (ACC), and the orbitofrontal cortex (OFC). The striatum has been implicated in integrating the signals from lower- and higher-level sensory cortex and transmitting the resultant signal to the frontal cortex [1]. The anterior cingulate and OFC have both been implicated in mediating different aspects of reward-related behaviors [2], as well as being crucial in decision making [3]. There are a number of other regions involved in rewards processing, each of which has received significant attention in the literature [4]. Many studies have been conducted in the animal model examining neurotransmitter transmission between these regions, particularly dopamine [5], and the connectivity pathways between the various involved regions are well established [6].

However, while the individual component nuclei and the axonal connections between these regions is well understood, functional connectivity between these regions is mostly unknown. Some studies have attempted to examine the function of particular subsets of the network using implanted electrodes [7], [8], but due to the invasive nature of such experiments, these studies have been limited mostly to the animal model. Additionally, while functional magnetic resonance imaging (fMRI) and positron emission spectroscopy (PET) have been used extensively to identify regions involved in rewards processing, fundamental limitations of these imaging modalities prevent them from being applicable in examining the interactions between these regions on the timescale of milliseconds.

There have been a number of methods suggested for detecting deep activity via electroencephalography (EEG) and magnetoencephalography (MEG). These methods include using a matched filter design [9], [10], the construction of a boundary element model (BEM) to assist with solving the inverse problem [11], [12], and utilizing previously implanted deep electrodes [13]. However, none of these methods were universally accepted. Utilizing a matched filter design requires knowledge of or assumptions regarding the signal of interest, which in many research applications is unavailable. Utilizing implanted electrodes, while feasible in patients being treated for epilepsy where such implants are more common, is unrealistic for most other research and clinical aplications. BEM construction requires a magnetic resonance imaging (MRI) scan of the subject, which also is not always available to the researcher. Additionally, any computations executed on the BEM are limited by the mesh density, and are by nature approximations of the true magnetic field. Construction of a superfine mesh can be prohibitively computationally expensive. The optimal deep activity detector would be an analytical tool—not limited by computational restrictions—which could be applied to any MEG dataset, regardless of sensor geometry or availability of external information.

The expanded signal space separation (exSSS) method [14] accomplishes these goals. By combining analytical signal processing techniques with the noise-reducing SSS algorithm, the exSSS method can be applied to any MEG dataset, regardless of acquisition details. In this paper, we will discuss the application of the exSSS method to our MEG dataset.

II. Methods

The exSSS method utilizes two previously published signal processing techniques to extract deep signals. These techniques are the SSS method and beamspace methods.

A. Signal Space Separation

The SSS noise-reduction method [15] utilizes a property of the MEG imaging system to separate noise internal to the head from noise external to the scanner [16], [17]. This is

This work was supported by NIMH Grant R90 DA023420

E. Y. Kanal is with Department of Bioengineering, University of Pittsburgh, Pittsburgh, PA 15213, USA eykanal@erikdev.com

M. Sun is with Department of Neurosurgery, University of Pittsburgh Medical Center, Pittsburgh, PA 15213, USA drsun@pitt.edu

T. E. Özkurt is with Institute for Clinical Neuroscience and Medical Psychology, Heinrich Heine-University, Duesseldorf, Germany tolga.oezkurt@med.uni-duesseldorf.de

W. Jia is with Department of Neurosurgery, University of Pittsburgh, Pittsburgh, PA 15213, USA jiawenyan@gmail.com

R. Sclabassi is with Computational Diagnostics, Inc., Pittsburgh, PA 15213, USA bobs@cdi.com

accomplished by noting that the MEG sensor array (i.e., the MEG helmet) can be modeled as a source-free sphere within our total source space. Considering the entire source space in spherical coordinates, we can thus separate our source space as sources internal to the sensor array—the brain and surrounding tissues—and sources external to the sensor array—the room, ambient lights, other external sources of noise—separated by a source-free shell, representing the MEG sensor array. One of the main advantages of SSS is that there are very few assumptions made about the magnetic sources; the only assumption is that there are no magnetic sources on the sphere defined by the sensor array.

Mathematically, we can model this as follows. Given Maxwell's equation for a quasi-static magnetic field, $\nabla \times \mathbf{B} = \mu \mathbf{J}$, we note that the sphere defining the sensor array is source-free, or $\mathbf{J} = 0$ at $r = R$, where R is the distance from the origin of the sphere defined by the sensor array to the sensor array perimiter. As such, Maxwell's equation can be represented as $\nabla \times \mathbf{B} = 0$. Using the identity $\nabla \times \nabla \Psi = 0$, we define

$$\mathbf{B} = -\mu_0 \nabla \Psi, \tag{1}$$

where Ψ is termed the scalar potential. Within the spherical domain, we separate $\Psi(\varphi, \theta, r) = \Phi(\varphi)\Theta(\theta)R(r)$ and solve the resultant harmonic equation. Substituting the result in (1), we obtain

$$\begin{aligned}\mathbf{B}(\mathbf{r}) &= -\mu_0 \sum_{l=0}^{\infty} \sum_{m=-l}^{l} \alpha_{lm} \frac{\boldsymbol{\nu}_{lm}(\theta, \varphi)}{r^{l+1}} \\ &\quad - \mu_0 \sum_{l=0}^{\infty} \sum_{m=-l}^{l} \beta_{lm} r^l \boldsymbol{\omega}_{lm}(\theta, \varphi) \\ &\equiv \mathbf{B}_\alpha(\mathbf{r}) + \mathbf{B}_\beta(\mathbf{r}),\end{aligned} \tag{2}$$

where $\boldsymbol{\nu}_{lm}(\theta, \varphi)$ and $\boldsymbol{\omega}_{lm}(\theta, \varphi)$ represent modified spherical harmonic functions, r represents the radius of the spherical model of the sensor array volume, and α_{lm} and β_{lm} are the multipole moments of the internal and external current sources respectively [15]. Note that the magnetic field $\mathbf{B}(\mathbf{r})$ is a function of both α_{lm} and β_{lm}; by simply dropping the second term on the right-hand side of (2) we modulate $\mathbf{B}$ to only depend on the internal signals, defined by the coefficients α_{lm}.

B. exSSS Overview

Using the SSS method, $\mathbf{B}$ can be separated into two components, $\mathbf{B}_\alpha$ and $\mathbf{B}_\beta$, as described in (2). The full details of this derivation can be found in [14], but a brief description follows. $\mathbf{B}_\alpha$ and $\mathbf{B}_\beta$ can be represented using leadfield-like notation,

$$\alpha_{lm} = \int_{v'} \boldsymbol{\lambda}^{\alpha}_{lm}(\mathbf{r}') \cdot \mathbf{J}_{\text{in}}(\mathbf{r}') dv', \tag{3}$$

where $\mathbf{J}_{\text{in}}$ represents the sources within the head (i.e., internal to the sensor array) and $\boldsymbol{\lambda}^{\alpha}_{lm}$ is a lead field-like vector directly related to the vector spherical harmonic function. In this manner, we can apply the beamspace method to the SSS α coefficients within $\mathbf{B}_\alpha$. This can formulated mathematically as

$$\max_{\mathbf{T}} \frac{\text{tr}(\mathbf{T}^{\text{T}} \mathbf{G}_d \mathbf{T})/v_d}{\text{tr}(\mathbf{T}^{\text{T}} \mathbf{G}_s \mathbf{T})/v_s}, \tag{4}$$

where $\mathbf{G}_s$ and $\mathbf{G}_d$ represents the Gram matrix corresponding to the superficial and deep sources, respectively, and v_s and v_d are constants used for normalization.

By solving this maximization problem we can construct the exSSS filter as follows:

$$(\tilde{\alpha}_{lm}) = \alpha_{lm} \frac{3}{2l+3} \frac{1}{R^3 - \hat{r}^3} \frac{R^{2l+3} - \hat{r}2l + 3}{\hat{r}^{2l}}, \tag{5}$$

where R represents the sensor array radius and $\hat{r}$ the radius of the deep portion of the brain where signal should be amplified. By modulating α_{lm} in this fashion, the MEG dataset is modified such that the deep signal is amplified and the superficial signal attenuated. Note that no explicit assumptions were made relative to the source coordinates, source waveforms, or the presence of external information regarding the physical structure of the source space (i.e., MRI-based BEM).

C. Behavioral Paradigm

Numerous behavioral paradigms have been designed to activate various components of the rewards network. For our study, we chose to replicate a recent gambling study by Liu et al [18]. His paradigm consisted of showing subjects a wager, giving an opportunity to bet or bank (save the wager to their total winnings) on the roll of a die, and then observe the outcome of the die roll. Note that this study design enables subjects "regret" for poor decisions (see Table I). When analyzing viewing the differential neural activation between perceived correct and perceived incorrect trials, Liu found strong, selective activation of the corticolimbic rewards pathway. We adapted this paradigm for our study. Our paradigm is in all ways identical to that described in [18], save for the response phase; whereas Liu and colleagues set the response phase to a constant two seconds due to limitations with fMRI, we advanced to the feedback screen as soon as a response was detected.

D. Data Collection & Analysis

We ran 6 subjects in our study, and data from one subject was eventually rejected due to significant uncorrectable sensor noise. All subjects signed informed consent forms. The study paradigm was written using EPrime Studio 1.1 (Psychology Software Tools; Pittsburgh, PA). Each subject completed 320 trials, with a single trial consisting of one "wager, decision, feedback, fixation" loop, as depicted in Fig.

TABLE I
SUMMARY OF POSSIBLE OUTCOMES FROM GAMBLING PARADIGM FROM THE POINT OF VIEW OF THE SUBJECT.

Perceived Correct	Perceived Incorrect
Bet & Win (earned $$)	Bet & Lose (lost $$)
Bank & Lose (avoided losing $$)	Bank & Win (could have won $$)

1. All data was recorded using the 306-sensor Elekta NeuroMag MEG system in the University of Pittsburgh Center for Advanced Brain Magnetic Source Imaging (CABMSI) with a recording frequency of 2 KHz. Each subject performed an average of 171 correct and 145 incorrect trials (st. dev. 6.34 and 5.85, respectively), with an average of four no-response (st. dev. 2.90).

MEG data analysis was completed using the MNE software package (Martinos Center for Biomedical Imaging; Massachusetts General Hospital, Bostonon, MA). For this analysis, we examined only the 1300 ms surrounding the button press indicating a decision to bet or bank (500 ms prior to 800 ms post-push), indicated in Fig. 1 by the shaded region. All data was averaged according to "perceived outcome", passed through a 1-40 Hz bandpass filter, processed with SSP [9] using vectors acquired by the scanner at runtime, passed through the SSS filter, differenced, and passed through the exSSS filter. The differencing here refers to subtracting the "perceived correct" condition from the "perceived incorrect" condition; this was done to eliminate activation common to both conditions.

The Elekta NeuroMag-306 system contains 102 magnetometers and 204 axial gradiometers. For the purposes of this study, we examined only the magnetometers. The rationale for this decision lies in the type of field detected by each. The magnetometer will detect any change in field strength, irrespective of changes elsewhere. Axial gradiometers measure differential activity between one side of the gradiometer and the other [19]. For most superficial sources, both types of sensors are appropriate, since the field change should correspond with the local magnetic field gradient. However, when detecting deep activity, the fields generated by the deep dipoles theoretically span the entire head; on hemisphere would be the positive side and the other the negative. Such a broad gradient would be difficult to detect on the local scale, while being easily visible in the magnetometers.

As can be seen in Fig. 2, no significant signal is visible on the traces unprocessed by the exSSS method (Fig. 2a, 2c), whereas the datasets processed by exSSS contain notable peaks at 220 (Fig. 2b) and 270 ms (Fig. 2d). We see peak and additional peak at approximately 130 ms (Figs. 2b, 2d). This peak was strongest in the occipital regions, corresponding with the viewing of the feedback screen. In such a case, the 220 and 270 ms peaks could likely correspond to striatal and orbitofrontal activation, respectively, occuring after processing via visual regions. This is bolstered by the finding in the mouse model that activation between the striatal and frontal regions is delayed by 80-160 ms [7]. These findings, as well as the approximate timepoint of the activation, persisted through all subjects.

Additionally, in the processed dataset, signal was mostly observed in the temporal and outer central regions of the dataset, with less signal on the midline (see Fig. 3). This pattern of activation led us to believe we are seeing the signature of a deeper dipole. Inasmuch as MEG imaging detects current dipoles, superficial dipoles often appear in magnetometer traces as a peak to one side of the dipole and a

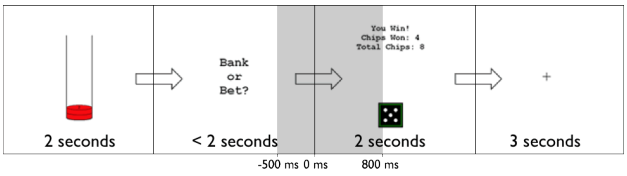

Fig. 1. Schematic of one trial from the gambling paradigm. Subjects view their ante for two seconds, have up to two seconds to respond, view the outcome for two seconds, and the fixation for three seconds. The area shaded in grey represents the 1300 ms surrounding the button press indicating a choice (500 ms prior and 800 ms following). This was the portion of the dataset which was analyzed in this study.

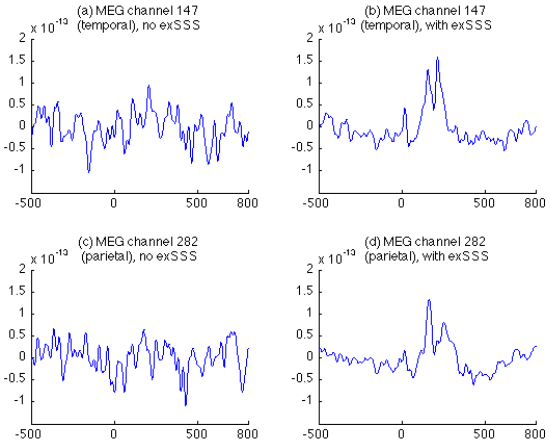

Fig. 2. Selected magnetometer channels from a single subject, both without and with exSSS processing. Note the visible peaks at 160 and 250 ms in the processed channels, neither of which were noticably present in the unprocessed data.

trough on the other. Seeing a peak appear on one hemisphere and a trough on the other suggests that we are seeing a dipole field pattern where the dipole is located close to the center of the brain.

To test whether the difference between the processed and unprocessed datasets is statistically significant, an F-test was conducted between the processed and unprocessed traces from dataset on a per-sensor basis. Significance in this test would imply that the information extracted using the exSSS algorithm was not visible in the unprocessed dataset. Of the 306 MEG magnetometers and gradiometers, over 90% were significantly different ($p < 0.001$). Of the remaining 10%, almost all were sensors located along the midline of the brain, where signal was weakest (see Fig. 3). This supports our hypothesis that data that was previously invisible has been extracted from this dataset using the exSSS method.

Note that there are two signals present in Fig. 3; a broad, tall peak/trough present bilaterally in the temporal regions, and a smaller, sharper peak present near the parietal/occipital border. The sharper peak occurs at approximately 130 ms after the onset of the feedback screen, suggesting that it may be an artifact of visual activity related to viewing and processing feedback information, and not related to the deeper signal which peaks approx 140 ms later, as described

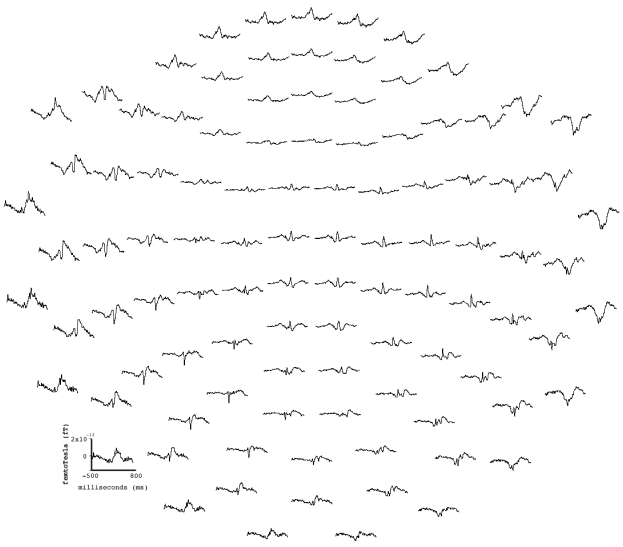

Fig. 3. A subset of the magnetometers from another subject. Note the presence of bilateral large signal shifts in the temporal regions;

above. Why such a visual signal would exist in differenced data, indicating a differentially strong visual signal during "correct" relative to "incorrect" trials, is unknown.

III. DISCUSSION

In this paper, we have described the application MEG and a novel signal processing technique (exSSS) to the problem of full-brain high-resolution temporal imaging of functional neural activity during human rewards processing. The results support the previous findings in the literature in demonstrating that the striatum is differentially activated during "correct" trials relative to "incorrect" trials. Addtionally, we have shown in the human model that there are likely two separate timpoints at which the deeper regions are activated, separated by 50 ms. These findings have previously been found in the rat model, and are suggestive of a recurrent network within the basal ganglia. This study did not utilize localization methods on the data; future studies should examine whether the activation patterns arising from localized data support the finding of a bimodal activity pattern.

More generally, these results suggest that through a combination of MEG and exSSS we can extract deep activity from an MEG dataset across subjects. As can be seen from the findings presented here, patterns previously uncovered using fMRI may likely contain details only visible using high-temporal imaging modalities such as MEG. There are many potential uses for this type of tool, but one particularly interesting use would be the application of inverse methods on the filtered dataset with the intent of extracting neural time courses for experimentally activated regions of interest. These regions could then be compared using a variety of time series analysis methods, which could shed significant light on the nature of network-level neural interactions.

IV. ACKNOWLEDGMENTS

We would like to acknowledge support from NIH/NIDA Grant R90 DA023420 and from Computational Diagnostics, Inc.. Additionally, we would like to thank the Center for Advanced Brain Magnetic Source Imaging (UPMC, Pittsburgh, PA) for the use of their MEG scanner, and the Magnetic Resonance Research Center (UPMC, Pittsburgh, PA) for the use of the MRI scanners.

REFERENCES

[1] P. R. Montague, S. E. Hyman, and J. D. Cohen, "Computational roles for dopamine in behavioural control," *Nature*, vol. 431, no. 7010, pp. 760–767, 10 2004/10/14/print.

[2] S. Hyman, R. Malenka, and E. Nestler, "Neural mechanisms of addiction: The role of reward-related learning and memory," *Annual Review of Neuroscience*, vol. 29, no. 1, pp. 565–598, 2006.

[3] D. Krawczyk, "Contributions of the prefrontal cortex to the neural basis of human decision making," *Neurosci Biobehav Rev*, vol. 26, no. 6, pp. 631–64, Oct 2002, 0149-7634 (Print) Journal Article Review.

[4] A. Graybiel, "The basal ganglia: learning new tricks and loving it," *Curr Opin Neurobiol*, vol. 15, no. 6, pp. 638–44, Dec 2005, 0959-4388 (Print) Journal Article Review.

[5] W. Schultz, "Getting formal with dopamine and reward," *Neuron*, vol. 36, no. 2, pp. 241–63, Oct 2002.

[6] P. Kalivas and N. Volkow, "The neural basis of addiction: A pathology of motivation and choice," *Am J Psychiatry*, vol. 162, no. 8, pp. 1403–1413, Aug 2005.

[7] M. Gao, C. Liu, S. Yang, G. Jin, B. Bunney, and W. Shi, "Functional coupling between the prefrontal cortex and dopamine neurons in the ventral tegmental area," *J Neurosci*, vol. 27, no. 20, pp. 5414–21, May 2007.

[8] W. Shi, "Slow oscillatory firing: a major firing pattern of dopamine neurons in the ventral tegmental area," *J Neurophysiol*, vol. 94, no. 5, pp. 3516–22, Nov 2005.

[9] C. D. Tesche, M. A. Uusitalo, R. J. Ilmoniemi, M. Huotilainen, M. Kajola, and O. Salonen, "Signal-space projections of meg data characterize both distributed and well-localized neuronal sources." *Electroencephalogr Clin Neurophysiol*, vol. 95, no. 3, pp. 189–200, 1995.

[10] C. D. Tesche, J. Karhu, and S. O. Tissari, "Non-invasive detection of neuronal population activity in human hippocampus." *Brain Res Cogn Brain Res*, vol. 4, no. 1, pp. 39–47, 1996.

[11] Y. Attal, M. Bhattacharjee, J. Yelnik, B. Cottereau, J. Lefevre, Y. Okada, E. Bardinet, M. Chupin, and S. Baillet, "Modeling and detecting deep brain activity with meg & eeg." *Conf Proc IEEE Eng Med Biol Soc*, vol. 1, pp. 4937–4940, 2007.

[12] L. Parkkonen and J. Mäkelä, "Meg sees deep sources: measuring and modelling brainstem auditory evoked potentials," *Proceedings of the 13th Int'l Conference on Biomagnetism, Jena*, 2002.

[13] R. C. Knowlton and J. Shih, "Magnetoencephalography in epilepsy." *Epilepsia*, vol. 45 Suppl 4, pp. 61–71, 2004.

[14] T. Ozkurt, M. Sun, and R. Sclabassi, "Decomposition of magnetoencephalographic data into components corresponding to deep and superficial sources," *Biomedical Engineering, IEEE Transactions on*, vol. 55, no. 6, pp. 1716–1727, June 2008.

[15] S. Taulu and M. Kajola, "Presentation of electromagnetic multichannel data: The signal space separation method," *Journal of Applied Physics*, vol. 97, no. 12, p. 124905, 2005.

[16] J. Nurminen, S. Taulu, and Y. Okada, "Effects of sensor calibration, balancing and parametrization on the signal space separation method," *Physics in Medicine and Biology*, vol. 53, no. 7, pp. 1975–1987, 2008.

[17] S. E. Taulu, J. Simola, and M. Kajola, "Applications of the signal space separation method," *IEEE Trans Sig Proc*, vol. 53, no. 9, pp. 3359–72, 2005.

[18] X. Liu, D. K. Powell, H. Wang, B. T. Gold, C. R. Corlby, and J. E. Joseph, "Functional dissociation in frontal and striatal areas for processing of positive and negative reward information," *J Neurosci*, vol. 27, no. 17, pp. 4587–4597, Apr 2007.

[19] M. Hamalainen, R. Hari, R. Ilmoniemi, J. Knuutila, and O. Lounasmaa, "Magnetoencephalography - theory, instrumentation, and applications to noninvasive studies of the working human brain," *Reviews of Modern Physics*, vol. 65, no. 2, pp. 413–497, 1993.